machines

Article

EHB Gear-Drive Symmetric Dead-Zone Finite-Time Adaptive Control

Shuai Wang, Qinghua Cao, Fukuo Ma and Jian Wu *

School of Automotive Engineering, Liaocheng University, Liaocheng 252000, China; ws15854393910@163.com (S.W.); 18353643398@163.com (Q.C.); 15552307021@163.com (F.M.)
* Correspondence: wujian@lcu.edu.cn

Abstract: Intelligent driving vehicles require more accurate and stable braking control. Electro-hydraulic braking (EHB) systems can better adapt to the development of autonomous driving technology. The gear transmission system plays a crucial role in EHB deceleration and torque increase mechanisms. However, its dead-zone nonlinearity poses challenges for EHB control. To address the position-control problem in the EHB gear transmission system, we propose a finite-time adaptive control method for the symmetrical dead zone. This approach combines adaptive control theory with finite-time control theory and designs parameter-updating laws for the unknown parameters in the system. Boundary estimates are introduced into the parameter-update laws and control laws to compensate for unknown disturbances. By adjusting the relevant parameters, the convergence rate can be improved, ensuring that errors converge within a specified range within a limited time. After modifying the parameter-updating laws and control laws, all closed-loop signals remain bounded. Finally, we validate the proposed control strategy through simulation and hardware-in-the-loop (HIL) testing. The results demonstrate that the control strategy developed in this study achieves high tracking accuracy and stability even in the presence of dead zones, unknown parameters, and unknown interferences in the EHB gear-drive servo system.

Keywords: adaptive control; finite-time control; symmetric dead-zone nonlinearity; gear transmission servosystems

Citation: Wang, S.; Cao, Q.; Ma, F.; Wu, J. EHB Gear-Drive Symmetric Dead-Zone Finite-Time Adaptive Control. *Machines* **2023**, *11*, 1002. https://doi.org/10.3390/machines11111002

Academic Editor: Domenico Mundo

Received: 13 September 2023
Revised: 19 October 2023
Accepted: 26 October 2023
Published: 30 October 2023

1. Introduction

With the development of intelligent vehicles and autonomous driving technology, braking systems are playing an increasingly important role. In order to improve the application of automatic driving technology in vehicles, a more reliable braking system has become a research hotspot for countless researchers [1–3]. In this context, EHB has gradually replaced traditional braking methods and been applied and promoted in intelligent vehicles due to its advantages such as simple structure, rapid response and strong compatibility [4–7]. With the continuous improvement of control accuracy requirements, the existence of gap nonlinearity has gradually been paid attention to [8,9].

Backlash nonlinearity is inevitable in many practical systems and it may seriously affect the dynamic performance, control accuracy and stability of the controlled system [10–12]. The gear group is an important part of the EHB deceleration and torque increase mechanism. The position-control accuracy of EHB gear-drive servo systems is seriously affected due to clearance, parameter uncertainty and interference [13]. Because of the nonlinear problem of gear backlash, the parameters of the system will change [14]. Because of the unknown time-varying disturbance, the position control of the EHB gear-drive servo system will be more difficult. Therefore, it is necessary to find a control method suitable for the nonlinear backlash of the EHB gear transmission system.

Many experts and scholars have embarked on research on the problem of backlash in the process of gear transmission. In practical engineering, the stiffness and moment of inertia of the gear-drive servo system are often considered. Therefore, the dead-zone model is often used to describe the backlash nonlinear problem of the gear-drive servo system. Within this system, the existence of a backlash problem will lead to the change of different parameters. Additionally, due to its non-differentiable characteristics, it will have an impact on position control [15]. In order to overcome the non-differentiable characteristics of the backlash nonlinearity in the gear transmission system, a new differentiable dead-zone model was established in the literature [16]. State feedback is used to transform it into a linear system, thus avoiding the complex model-switching system and inverse model compensation. The output tracking problem of the gear-drive servo system is realized. In reference [17], the author proposes an inversion algorithm based on a differentiable dead-zone model. The non-differentiable characteristic of the dead-zone model is overcome; the backlash nonlinearity is eliminated and the high-precision output tracking is realized. Papers [18,19], respectively, put forward a differentiable dead-zone model for the gear-drive servo system to solve the output-control problem and verify the effectiveness of the controller through simulation. However, the above method is only applicable to the determination of dead-zone model parameters, which obviously makes it difficult to meet the above conditions in actual working conditions.

An EHB gear-drive servo system will inevitably change the system parameters due to various factors in the working process, which presents challenges in accurate output position tracking. Researchers at the University of Texas designed a dead-zone compensator based on a fuzzy logic controller for the dead-zone model with unknown system parameters. By designing the optimization algorithm of fuzzy logic parameters, small tracking error and bounded parameter estimation are guaranteed [20]. In reference [21], the author designed an adaptive controller by introducing a smooth inverse function of dead interval for the unknown dead interval nonlinearity of uncertain systems. The stability and transient performance of the system are guaranteed. In reference [22], the author uses fuzzy logic to identify unknown nonlinear functions. An adaptive fuzzy output feedback control method is proposed, which ensures the control precision and the stability of the closed-loop system. The unknown disturbance will inevitably exist in the actual system, which will affect the control precision. Some scholars compensate for the influence of unknown disturbance by disturbance observer or adversarial attack [23–25]. The authors of reference [26] further consider the influence of unknown perturbations while considering unknown parameters. By adding a robust term to the parameter-updating laws, the authors effectively compensate for the effect of unknown interference. In reference [27], the author proposed a linear nonsingular transformation of state variables and designed an adaptive controller for gear transmission systems. The tracking performance can be guaranteed in the case of parameter uncertainty and unknown disturbance. Therefore, according to the above analysis, the adaptive control algorithm is a good solution for the unknown parameters of the dead-zone model and the unknown disturbance [28,29].

Based on the above analysis, it is necessary to consider the influence of unknown system parameters and disturbance for the output position-tracking control of the gear-drive servo system. In the actual EHB condition, the influence of system stability and convergence rate should also be considered. In reference [30], the authors consider the problem that each subsystem has dead input and is not modeled. A decentralized finite-time controller based on recursion is designed, which makes all state variables return to zero in finite time. The controller designed by the author can ensure the stability of the system in fixed time, in which the stability time depends on the design parameters of the control system. In literature [31], the authors further consider the uncertainty and time delay of system parameters on the basis of the dead-zone problem. In this paper, an adaptive finite-time control scheme is proposed to solve the uncertainty and unknown nonlinearity of the system with neural network. In reference [32], the author proposed an adaptive finite-time control scheme. By designing an adaptive dummy variable, an adaptive law and a controller, the error is guaranteed to converge to a certain range in a certain time. Therefore, the combination of an adaptive control algorithm and finite-time control algorithm can effectively improve the control accuracy and convergence rate of a gear-drive servo system with unknown parameters, unknown disturbance and dead-zone problems.

Based on the above analysis, the dead zone will inevitably exist in the EHB gear-drive servo system, which will affect the precision of position control. System parameters may change due to the dead-zone problem. At the same time, the influence of the unknown disturbance and the convergence rate of the system should be considered. Therefore, on the basis of the above content in this paper, a finite-time adaptive control strategy for a symmetrical dead zone of EHB gear transmission is proposed. The contributions are as follows:

(1) The unknown disturbance and parameter uncertainty of the EHB gear-drive servo system are considered. In this paper, the parameter-updating law is designed for each parameter in view of the parameter uncertainty in the system. In order to compensate for the unknown disturbance, the boundary estimates are introduced into the parameter-updating law and the control law.

(2) In order to improve the convergence rate of the system, this paper combines the adaptive control theory with the finite-time control theory to introduce the power exponent β. By adjusting the value of β, the system error can be guaranteed to converge to a certain range in a limited time.

The rest of this article is arranged as follows. In Section 2, the position-control problem of an EHB gear-drive servo system with symmetric dead-zone nonlinearity is described. In Section 3, based on the above problems, a finite-time adaptive controller is designed, its stability is analyzed, and the reliability of the controller is proved. The simulation is verified in Section 4, and the HIL test is carried out in Section 5. Finally, the article is summarized in Section 6.

2. System Modeling

The EHB structure is shown in Figure 1. An EHB system is mainly composed of a brake pedal, a pedal stroke sensor, a transmission mechanism, a power source, an oil storage pot and a brake master cylinder. The gear-drive servo system is an important part of the transmission mechanism. The pinion of the gear-drive servo system is connected to the power source, and the big gear is connected with the motion-conversion mechanism, which plays the role of slowing down and increasing torque; it is an important part of EHB. The existence of a dead-zone problem will affect the position-control accuracy of the gear-drive servo system and then affect the pressure control of the EHB brake master cylinder, thus affecting the braking effect. Therefore, the existence of the dead-zone problem will pose a threat to vehicle safety and become a factor that cannot be ignored in the development process of intelligent vehicles.

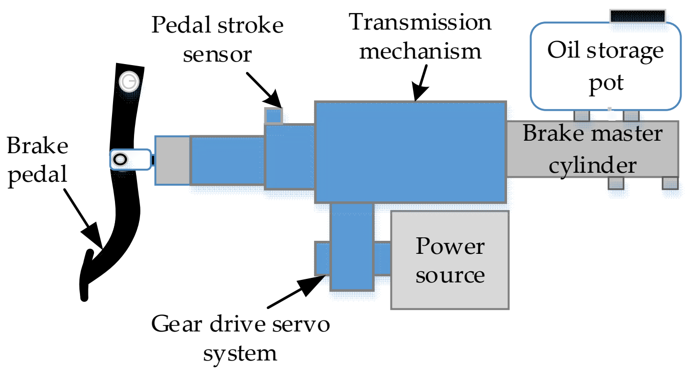

Figure 1. EHB structure diagram.

The symmetric dead zone of EHB gear transmission considered in this paper is shown in Figure 2.

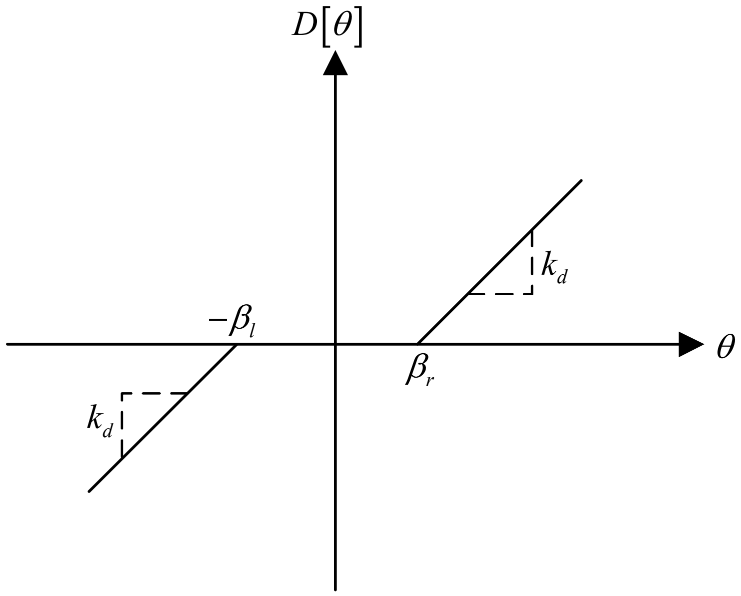

Figure 2. Symmetry dead zone.

The EHB gear-drive servo system is as follows [33]:

$$\begin{cases} J_l\ddot{\theta}_l + C_l\dot{\theta}_l = iD[\theta] \\ J_m\ddot{\theta}_m + C_m\dot{\theta}_m = u - D[\theta] \end{cases} \tag{1}$$

Among them, J_l, θ_l and C_l are the moment of inertia, position and viscous friction coefficient of the driven side gear, respectively. J_m, θ_m and C_m are the moment of inertia, position and viscous friction coefficient of the driving side gear, respectively. i is the transmission ratio, u is the input torque, θ is the relative displacement ($\theta = \theta_m - i\theta_l$), $D[\theta]$ is the transmission torque.

Transmission torque $D[\theta]$ is defined as:

$$D[\theta] = \begin{cases} k_d(\theta - \beta_r), & if \quad \theta \geq \beta_r \\ 0, & if \quad -\beta_l < \theta < \beta_r \\ k_d(\theta + \beta_l), & if \quad \theta \leq -\beta_l \end{cases} \tag{2}$$

Among them, $k_d > 0$ denotes the stiffness coefficient and $\beta_r > 0$, $\beta_l > 0$ denote the break points.

Remark 1. *The parameters J_m, θ_m, C_m, J_l, θ_l, C_l, k_d, β_r and β_l are unknown in the system. The control objective is to adjust the position of the driven side to the ideal position while ensuring the boundedness of all closed-loop signals.*

To deal with the effects caused by symmetry dead zones, rewrite $D[\theta]$ as:

$$D[\theta] = k_d\theta + \Delta d[\theta] \tag{3}$$

Among them,

$$\Delta d[\theta] = \begin{cases} -k_d\beta_r, & if \quad \theta \geq \beta_r \\ -k_d\theta, & if \quad -\beta_l < \theta < \beta_r \\ k_d\beta_l, & if \quad \theta \leq -\beta_l \end{cases} \tag{4}$$

It can be concluded that:

$$|\Delta d[\theta]| \leq k_d\overline{\beta} \tag{5}$$

Among them, $\overline{\beta} = \max\{\beta_r, \beta_l\}$.

Let $x_1 = \theta_l$, $x_2 = \dot{\theta}_l$, $x_3 = \theta_m$, $x_4 = \dot{\theta}_m$, $a_1 = ik_d/J_l$, $a_2 = i^2k_d/J_l$, $a_3 = C_l/J_l$, $b_1 = ik_d/J_m$, $b_2 = k_d/J_m$, $b_3 = C_m/J_m$, $b_4 = 1/J_m$, $d_1 = i\Delta d[\theta]/J_l$, $d_2 = -\Delta d[\theta]/J_m$. Finally, the following feedback system is established:

$$\begin{cases} \dot{x}_1 = x_2 \\ \dot{x}_2 = a_1x_3 - a_2x_1 - a_3x_2 + d_1 \\ \dot{x}_3 = x_4 \\ \dot{x}_4 = b_1x_1 - b_2x_3 - b_3x_4 + d_2 + b_4u \end{cases} \tag{6}$$

Among them,

$$d_1 \leq \frac{ik_d}{J_l}\overline{\beta} \leq D_1 \tag{7}$$

$$d_2 \leq \frac{k_d}{J_m}\overline{\beta} \leq D_2 \tag{8}$$

where d_1 and d_2 are additional disturbances.

Remark 2. *The system will be subject to unknown interference in actual operation, such as vibration and temperature change. These unknown disturbances may cause changes in system parameters and affect preset dead-zone breakpoints. As shown in Equations (6)–(8), there are set bounded values for additional disturbances d_1 and d_2 to compensate for the effects of disturbances.*

3. Controller Designing and Stability Analysis

The control logic block diagram is shown in Figure 3.

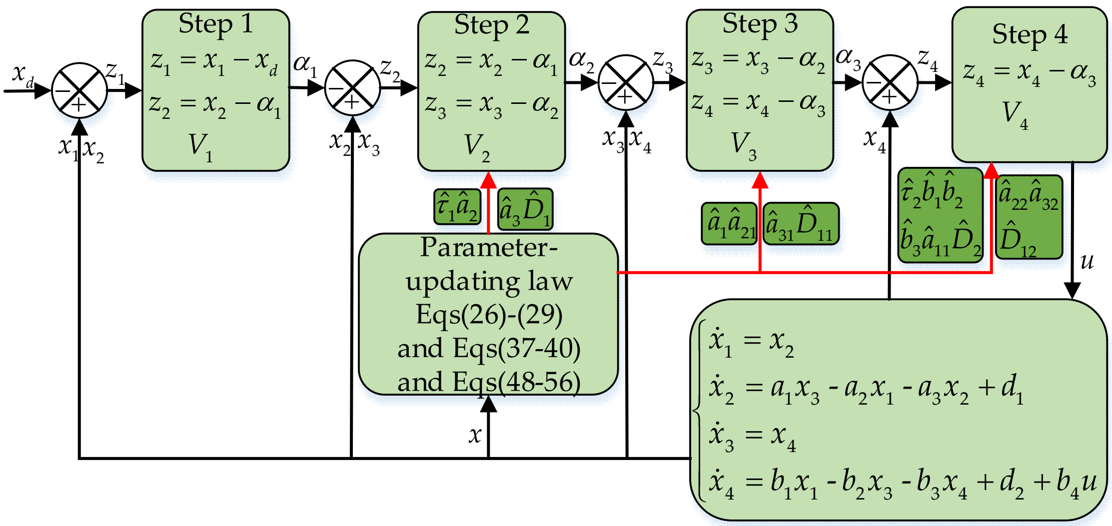

Figure 3. Control logic block diagram.

3.1. Design of Adaptive Controller

The multi-variable EHB gear-drive servo system is decomposed into several subsystems. The Lyapunov function of each step is constructed in the design process, and the parameter-updating law and control law are solved. Ensure that the position x_1 of the driven gear keeps track of the expected value x_d.

Step 1: First, construct the following error:

$$z_1 = x_1 - x_d \tag{9}$$

$$z_2 = x_2 - \alpha_1 \tag{10}$$

Among them, α_1 is the control law to be designed in this step.
Taking the derivative of z_1 gives us:

$$\dot{z}_1 = z_2 + \alpha_1 - \dot{x}_d \tag{11}$$

Design the Lyapunov function for this step.

$$V_1 = \frac{1}{2} z_1^2 \tag{12}$$

So,

$$\dot{V}_1 = z_1 \left(z_2 + \alpha_1 - \dot{x}_d \right) \tag{13}$$

Design control law α_1 is:

$$\alpha_1 = -\lambda_1 z_1^{2\beta - 1} - s_1 z_1 + \dot{x}_d \tag{14}$$

Among them, λ_1 and s_1 are normal numbers, and $0 < \beta < 1$.

$$\dot{V}_1 = -\lambda_1 z_1^{2\beta} - s_1 z_1^2 + z_1 z_2 \tag{15}$$

Step 2: Construct the error of this step.

$$z_3 = x_3 - \alpha_2 \tag{16}$$

From Equations (10), (14) and (16), we can get:

$$\dot{z}_2 = a_1 z_3 + a_1 \alpha_2 - a_2 x_1 - a_3 x_2 + d_1 - \frac{\partial \alpha_1}{\partial x_1} x_2 - \frac{\partial \alpha_1}{\partial x_d} \dot{x}_d - \frac{\partial \alpha_1}{\partial \dot{x}_d} \ddot{x}_d \tag{17}$$

Let

$$\tau_1 = \frac{1}{a_1} \tag{18}$$

$$\alpha_2 = \hat{\tau}_1 \overline{\alpha}_2 \tag{19}$$

So, design $\overline{\alpha}_2$ is:

$$\overline{\alpha}_2 = -z_1 - \lambda_2 z_2^{2\beta - 1} - s_2 z_2 + \hat{a}_2 x_1 + \hat{a}_3 x_2 - \tanh\left(\frac{z_2}{\varepsilon_1} \right) \hat{D}_1 + \frac{\partial \alpha_1}{\partial x_1} x_2 + \frac{\partial \alpha_1}{\partial x_d} \dot{x}_d + \frac{\partial \alpha_1}{\partial \dot{x}_d} \ddot{x}_d \tag{20}$$

Among them, λ_2 and s_2 are normal numbers, $\hat{a}_2$ is the estimate of a_2, $\hat{a}_3$ is the estimate of a_3, $\hat{D}_1$ is the estimate of D_1, ε_1 is an arbitrary normal number.

The Lyapunov function for constructing this step is:

$$V_2 = V_1 + \frac{1}{2} z_2^2 + \frac{a_1}{2\gamma_1} \widetilde{\tau}_1^2 + \frac{1}{2\gamma_2} \widetilde{a}_2^2 + \frac{1}{2\gamma_3} \widetilde{a}_3^2 + \frac{1}{2\gamma_4} \widetilde{D}_1^2 \tag{21}$$

Among them: $\gamma_1 - \gamma_4$ is a normal number, $\widetilde{\tau}_1 = \tau_1 - \hat{\tau}_1$, $\widetilde{a}_2 = a_2 - \hat{a}_2$, $\widetilde{a}_3 = a_3 - \hat{a}_3$, $\widetilde{D}_1 = D_1 - \hat{D}_1$.

Taking the derivative of V_2 gives us:

$$\begin{aligned} \dot{V}_2 = -\lambda_1 z_1^{2\beta} - s_1 z_1^2 + z_1 z_2 + z_2 (a_1 z_3 + \overline{\alpha}_2 - a_1 \widetilde{\tau}_1 \overline{\alpha}_2 - a_2 x_1 - a_3 x_2 + d_1 - \tfrac{\partial \alpha_1}{\partial x_1} x_2 - \tfrac{\partial \alpha_1}{\partial x_d} \dot{x}_d \\ - \tfrac{\partial \alpha_1}{\partial \dot{x}_d} \ddot{x}_d) - \tfrac{a_1}{\gamma_1} \widetilde{\tau}_1 \dot{\hat{\tau}}_1 - \tfrac{1}{\gamma_2} \widetilde{a}_2 \dot{\hat{a}}_2 - \tfrac{1}{\gamma_3} \widetilde{a}_3 \dot{\hat{a}}_3 - \tfrac{1}{\gamma_4} \widetilde{D}_1 \dot{\hat{D}}_1 \end{aligned} \tag{22}$$

It can be obtained from Equation (20):

$$\begin{aligned}\dot{V}_2 &= -\lambda_1 z_1^{2\beta} - \lambda_2 z_2^{2\beta} - s_1 z_1^2 - s_2 z_2^2 + a_1 z_2 z_3 - z_2 a_1 \widetilde{\tau}_1 \overline{\alpha}_2 + z_2 \widetilde{a}_2 x_1 + z_2 \widetilde{a}_3 x_2 \\ &+ z_2 d_1 - z_2 \tanh(\tfrac{z_2}{\varepsilon_1}) \hat{D}_1 - \tfrac{a_1}{\gamma_1} \widetilde{\tau}_1 \dot{\hat{\tau}}_1 - \tfrac{1}{\gamma_2} \widetilde{a}_2 \dot{\hat{a}}_2 - \tfrac{1}{\gamma_3} \widetilde{a}_3 \dot{\hat{a}}_3 - \tfrac{1}{\gamma_4} \widetilde{D}_1 \dot{\hat{D}}_1 \\ &\leq -\lambda_1 z_1^{2\beta} - \lambda_2 z_2^{2\beta} - s_1 z_1^2 - s_2 z_2^2 + a_1 z_2 z_3 - z_2 a_1 \widetilde{\tau}_1 \overline{\alpha}_2 + z_2 \widetilde{a}_2 x_1 + z_2 \widetilde{a}_3 x_2 \\ &+ \left[|z_2| - z_2 \tanh(\tfrac{z_2}{\varepsilon_1}) \right] D_1 + z_2 \tanh(\tfrac{z_2}{\varepsilon_1}) \widetilde{D}_1 - \tfrac{a_1}{\gamma_1} \widetilde{\tau}_1 \dot{\hat{\tau}}_1 - \tfrac{1}{\gamma_2} \widetilde{a}_2 \dot{\hat{a}}_2 - \tfrac{1}{\gamma_3} \widetilde{a}_3 \dot{\hat{a}}_3 - \tfrac{1}{\gamma_4} \widetilde{D}_1 \dot{\hat{D}}_1\end{aligned} \tag{23}$$

The following inequality applies to any $\varphi > 0$ and $\varphi \in R$ [34–36].

$$0 \leq |\varphi| - \varphi \tanh(\frac{\varphi}{\varepsilon}) \leq 0.2785\varepsilon \tag{24}$$

where φ is a constant, and $\varphi = e^{-(\varphi+1)}$. And that gives us $\varphi = 0.2785$.

So, Formula (23) becomes:

$$\begin{aligned}\dot{V}_2 &\leq -\lambda_1 z_1^{2\beta} - \lambda_2 z_2^{2\beta} - s_1 z_1^2 - s_2 z_2^2 + a_1 z_2 z_3 + 0.2785\varepsilon_1 D_1 - z_2 a_1 \widetilde{\tau}_1 \overline{\alpha}_2 + z_2 \widetilde{a}_2 x_1 \\ &+ z_2 \widetilde{a}_3 x_2 + z_2 \tanh(\tfrac{z_2}{\varepsilon_1}) \widetilde{D}_1 - \tfrac{a_1}{\gamma_1} \widetilde{\tau}_1 \dot{\hat{\tau}}_1 - \tfrac{1}{\gamma_2} \widetilde{a}_2 \dot{\hat{a}}_2 - \tfrac{1}{\gamma_3} \widetilde{a}_3 \dot{\hat{a}}_3 - \tfrac{1}{\gamma_4} \widetilde{D}_1 \dot{\hat{D}}_1 \\ &= -\lambda_1 z_1^{2\beta} - \lambda_2 z_2^{2\beta} - s_1 z_1^2 - s_2 z_2^2 + a_1 z_2 z_3 + 0.2785\varepsilon_1 D_1 + \tfrac{a_1}{\gamma_1} \widetilde{\tau}_1 (-z_2 \gamma_1 \overline{\alpha}_2 - \dot{\hat{\tau}}_1) \\ &+ \tfrac{1}{\gamma_2} \widetilde{a}_2 (z_2 \gamma_2 x_1 - \dot{\hat{a}}_2) + \tfrac{1}{\gamma_3} \widetilde{a}_3 (z_2 \gamma_3 x_2 - \dot{\hat{a}}_2) + \tfrac{1}{\gamma_4} \widetilde{D}_1 [z_2 \gamma_4 \tanh(\tfrac{z_2}{\varepsilon_1}) - \dot{\hat{D}}_1]\end{aligned} \tag{25}$$

According to Equation (25), the updating laws of design parameters is shown as follows:

$$\dot{\hat{\tau}}_1 = -z_2 \gamma_1 \overline{\alpha}_2 + \gamma_1 \lambda_3 \widetilde{\tau}_1^{2\beta-1} + \gamma_1 s_3 \widetilde{\tau}_1 \tag{26}$$

$$\dot{\hat{a}}_2 = z_2 \gamma_2 x_1 + \gamma_2 \lambda_4 \widetilde{a}_2^{2\beta-1} + \gamma_2 s_4 \widetilde{a}_2 \tag{27}$$

$$\dot{\hat{a}}_3 = z_2 \gamma_3 x_2 + \gamma_3 \lambda_5 \widetilde{a}_3^{2\beta-1} + \gamma_3 s_5 \widetilde{a}_3 \tag{28}$$

$$\dot{\hat{D}}_1 = z_2 \gamma_4 \tanh(\frac{z_2}{\varepsilon_1}) + \gamma_4 \lambda_6 \widetilde{D}_1^{2\beta-1} - \gamma_4 s_6 \widetilde{D}_1 \tag{29}$$

Combining Formula (26)–(29), Formula (25) becomes:

$$\begin{aligned}\dot{V}_2 \leq -\lambda_1 z_1^{2\beta} - \lambda_2 z_2^{2\beta} - a_1 \lambda_3 \widetilde{\tau}_1^{2\beta} - \lambda_4 \widetilde{a}_2^{2\beta} - \lambda_5 \widetilde{a}_3^{2\beta} - \lambda_6 \widetilde{D}_1^{2\beta} - s_1 z_1^2 - s_2 z_2^2 - a_1 s_3 \widetilde{\tau}_1^2 - s_4 \widetilde{a}_2^2 \\ -s_5 \widetilde{a}_3^2 - s_6 \widetilde{D}_1^2 + a_1 z_2 z_3 + 0.2785\varepsilon_1 D_1\end{aligned} \tag{30}$$

Step 3: The error of constructing this step is:

$$z_4 = x_4 - \alpha_3 \tag{31}$$

From Formulas (6), (14), (16) and (18)–(20), we can obtain:

$$\dot{z}_3 = z_4 + \alpha_3 - a_1 \frac{\partial \alpha_2}{\partial x_2} x_3 + a_2 \frac{\partial \alpha_2}{\partial x_2} x_1 + a_3 \frac{\partial \alpha_2}{\partial x_2} x_2 + \frac{\partial \alpha_2}{\partial x_2} d_1 - H_1 \tag{32}$$

Among them,

$$H_1 = \frac{\partial \alpha_2}{\partial x_1} x_2 + \frac{\partial \alpha_2}{\partial \hat{\tau}_1} \dot{\hat{\tau}}_1 + \frac{\partial \alpha_2}{\partial \hat{D}_1} \dot{\hat{D}}_1 + \frac{\partial \alpha_2}{\partial x_d} \dot{x}_d + \frac{\partial \alpha_2}{\partial \dot{x}_d} \ddot{x}_d + \frac{\partial \alpha_2}{\partial \ddot{x}_d} \dddot{x}_d \tag{33}$$

Construct the Lyapunov function as follows:

$$V_3 = V_2 + \frac{1}{2} z_3^2 + \frac{1}{2\gamma_5} \widetilde{a}_1^2 + \frac{1}{2\gamma_6} \widetilde{a}_{21}^2 + \frac{1}{2\gamma_7} \widetilde{a}_{31}^2 + \frac{1}{2\gamma_8} \widetilde{D}_{11}^2 \tag{34}$$

Among them, $\gamma_5 - \gamma_8$ are the normal number, $\widetilde{a}_1 = a_1 - \hat{a}_1$, $\widetilde{a}_{21} = a_2 - \hat{a}_{21}$, $\widetilde{a}_{31} = a_3 - \hat{a}_{31}$, $\widetilde{D}_{11} = D_1 - \hat{D}_{11}$.

Design control law:

$$\begin{aligned} \alpha_3 = -\hat{a}_1 z_2 - \lambda_7 z_3^{2\beta-1} - s_7 z_3 + \hat{a}_1 \tfrac{\partial\alpha_2}{\partial x_2} x_3 - \hat{a}_{21} \tfrac{\partial\alpha_2}{\partial x_2} x_1 - \hat{a}_{31} \tfrac{\partial\alpha_2}{\partial x_2} x_2 \\ - \tfrac{\partial\alpha_2}{\partial x_2} \tanh[\tfrac{(\partial\alpha_2/\partial x_2) z_3}{\varepsilon_2}] \hat{D}_{11} + H_1 \end{aligned} \tag{35}$$

Among them, λ_7 and s_7 are normal numbers, $\hat{a}_1$ is the estimate of a_1, $\hat{a}_{21}$ is the estimate of a_2, $\hat{a}_{31}$ is the estimate of a_3, $\hat{D}_{11}$ is the estimate of D_1, ε_2 is an arbitrary normal number.

According to Formulas (31)–(35), the following can be obtained:

$$\begin{aligned} \dot{V}_3 \leq\; & -\lambda_1 z_1^{2\beta} - \lambda_2 z_2^{2\beta} - a_1 \lambda_3 \widetilde{\tau}_1^{2\beta} - \lambda_4 \widetilde{a}_2^{2\beta} - \lambda_5 \widetilde{a}_3^{2\beta} - \lambda_6 \widetilde{D}_1^{2\beta} - \lambda_7 z_3^{2\beta} - s_1 z_1^2 \\ & - s_2 z_2^2 - a_1 s_3 \widetilde{\tau}_1^2 - s_4 \widetilde{a}_2^2 - s_5 \widetilde{a}_3^2 - s_6 \widetilde{D}_1^2 - s_7 z_3^2 + z_3 z_4 + 0.2785 \varepsilon_1 D_1 + \widetilde{a}_1 z_2 z_3 \\ & - z_3 \widetilde{a}_1 \tfrac{\partial\alpha_2}{\partial x_2} x_3 + z_3 \widetilde{a}_{21} \tfrac{\partial\alpha_2}{\partial x_2} x_1 + z_3 \widetilde{a}_{31} \tfrac{\partial\alpha_2}{\partial x_2} x_2 - \tfrac{\partial\alpha_2}{\partial x_2} z_3 \tanh[\tfrac{(\partial\alpha_2/\partial x_2) z_3}{\varepsilon_2}] \hat{D}_{11} \\ & + \tfrac{\partial\alpha_2}{\partial x_2} z_3 D_1 - \tfrac{1}{\gamma_5} \widetilde{a}_1 \dot{\hat{a}}_1 - \tfrac{1}{\gamma_6} \widetilde{a}_{21} \dot{\hat{a}}_{21} - \tfrac{1}{\gamma_7} \widetilde{a}_{31} \dot{\hat{a}}_{31} - \tfrac{1}{\gamma_8} \widetilde{D}_{11} \dot{\hat{D}}_{11} \\ & \leq -\lambda_1 z_1^{2\beta} - \lambda_2 z_2^{2\beta} - a_1 \lambda_3 \widetilde{\tau}_1^{2\beta} - \lambda_4 \widetilde{a}_2^{2\beta} - \lambda_5 \widetilde{a}_3^{2\beta} - \lambda_6 \widetilde{D}_1^{2\beta} - \lambda_7 z_3^{2\beta} - s_1 z_1^2 - s_2 z_2^2 \\ & - a_1 s_3 \widetilde{\tau}_1^2 - s_4 \widetilde{a}_2^2 - s_5 \widetilde{a}_3^2 - s_6 \widetilde{D}_1^2 - s_7 z_3^2 + z_3 z_4 + 0.2785 \varepsilon_1 D_1 + \widetilde{a}_1 z_2 z_3 - z_3 \widetilde{a}_1 \tfrac{\partial\alpha_2}{\partial x_2} x_3 \\ & + z_3 \widetilde{a}_{21} \tfrac{\partial\alpha_2}{\partial x_2} x_1 + z_3 \widetilde{a}_{31} \tfrac{\partial\alpha_2}{\partial x_2} x_2 + \left\{ \left| \tfrac{\partial\alpha_2}{\partial x_2} z_3 \right| - \tfrac{\partial\alpha_2}{\partial x_2} z_3 \tanh[\tfrac{(\partial\alpha_2/\partial x_2) z_3}{\varepsilon_2}] \right\} D_1 \\ & + \tfrac{\partial\alpha_2}{\partial x_2} z_3 \tanh[\tfrac{(\partial\alpha_2/\partial x_2) z_3}{\varepsilon_2}] \widetilde{D}_{11} - \tfrac{1}{\gamma_5} \widetilde{a}_1 \dot{\hat{a}}_1 - \tfrac{1}{\gamma_6} \widetilde{a}_{21} \dot{\hat{a}}_{21} - \tfrac{1}{\gamma_7} \widetilde{a}_{31} \dot{\hat{a}}_{31} - \tfrac{1}{\gamma_8} \widetilde{D}_{11} \dot{\hat{D}}_{11} \\ & \leq -\lambda_1 z_1^{2\beta} - \lambda_2 z_2^{2\beta} - a_1 \lambda_3 \widetilde{\tau}_1^{2\beta} - \lambda_4 \widetilde{a}_2^{2\beta} - \lambda_5 \widetilde{a}_3^{2\beta} - \lambda_6 \widetilde{D}_1^{2\beta} - \lambda_7 z_3^{2\beta} \\ & - s_1 z_1^2 - s_2 z_2^2 - a_1 s_3 \widetilde{\tau}_1^2 - s_4 \widetilde{a}_2^2 - s_5 \widetilde{a}_3^2 - s_6 \widetilde{D}_1^2 - s_7 z_3^2 + z_3 z_4 + 0.2785(\varepsilon_1 + \varepsilon_2) D_1 \\ & + \tfrac{1}{\gamma_5} \widetilde{a}_1 (\gamma_5 z_2 z_3 - \gamma_5 z_3 \tfrac{\partial\alpha_2}{\partial x_2} x_2 - \dot{\hat{a}}_1) + \tfrac{1}{\gamma_6} \widetilde{a}_{21} (\gamma_6 z_3 \tfrac{\partial\alpha_2}{\partial x_2} x_1 - \dot{\hat{a}}_{21}) \\ & + \tfrac{1}{\gamma_7} \widetilde{a}_{31} (\gamma_7 z_3 \tfrac{\partial\alpha_2}{\partial x_2} x_2 - \dot{\hat{a}}_{31}) + \tfrac{1}{\gamma_8} \widetilde{D}_{11} \left\{ \gamma_8 \tfrac{\partial\alpha_2}{\partial x_2} z_3 \tanh[\tfrac{(\partial\alpha_2/\partial x_2) z_3}{\varepsilon_2}] - \dot{\hat{D}}_{11} \right\} \end{aligned} \tag{36}$$

Updating the laws of design parameters is shown as follows:

$$\dot{\hat{a}}_1 = \gamma_5 z_2 z_3 - \gamma_5 z_3 \frac{\partial\alpha_2}{\partial x_2} x_2 + \gamma_5 \lambda_8 \widetilde{a}_1^{2\beta-1} + \gamma_5 s_8 \widetilde{a}_1 \tag{37}$$

$$\dot{\hat{a}}_{21} = \gamma_6 z_3 \frac{\partial\alpha_2}{\partial x_2} x_1 + \gamma_6 \lambda_9 \widetilde{a}_{21}^{2\beta-1} + \gamma_6 s_9 \widetilde{a}_{21} \tag{38}$$

$$\dot{\hat{a}}_{31} = \gamma_7 z_3 \frac{\partial\alpha_2}{\partial x_2} x_2 + \gamma_7 \lambda_{10} \widetilde{a}_{31}^{2\beta-1} + \gamma_7 s_{10} \widetilde{a}_{31} \tag{39}$$

$$\dot{\hat{D}}_{11} = \gamma_8 \frac{\partial\alpha_2}{\partial x_2} z_3 \tanh[\frac{(\partial\alpha_2/\partial x_2) z_3}{\varepsilon_2}] + \gamma_8 \lambda_{11} \widetilde{D}_{11}^{2\beta-1} + \gamma_8 s_{11} \widetilde{D}_{11} \tag{40}$$

Then, Formula (36) becomes:

$$\begin{aligned} \dot{V}_3 \leq\; & -\lambda_1 z_1^{2\beta} - \lambda_2 z_2^{2\beta} - a_1 \lambda_3 \widetilde{\tau}_1^{2\beta} - \lambda_4 \widetilde{a}_2^{2\beta} - \lambda_5 \widetilde{a}_3^{2\beta} - \lambda_6 \widetilde{D}_1^{2\beta} - \lambda_7 z_3^{2\beta} \\ & - \lambda_8 \widetilde{a}_1^{2\beta} - \lambda_9 \widetilde{a}_{21}^{2\beta} - \lambda_{10} \widetilde{a}_{31}^{2\beta} - \lambda_{11} \widetilde{D}_{11}^{2\beta} - s_1 z_1^2 - s_2 z_2^2 - a_1 s_3 \widetilde{\tau}_1^2 - s_4 \widetilde{a}_2^2 \\ & - s_5 \widetilde{a}_3^2 - s_6 \widetilde{D}_1^2 - s_7 z_3^2 - s_8 \widetilde{a}_1^2 - s_9 \widetilde{a}_{21}^2 - s_{10} \widetilde{a}_{31}^2 - s_{11} \widetilde{D}_{11}^2 + z_3 z_4 + 0.2785(\varepsilon_1 + \varepsilon_2) D_1 \end{aligned} \tag{41}$$

Step 4: Finally, deal with the last differential equation in Equation (6). According to Formulas (6) and (31), the following can be obtained.

$$\dot{z}_4 = b_1 x_1 - b_2 x_3 - b_3 x_4 + d_2 + b_4 u - a_1 \frac{\partial \alpha_3}{\partial x_2} x_3 + a_2 \frac{\partial \alpha_3}{\partial x_2} x_1 + a_3 \frac{\partial \alpha_3}{\partial x_2} x_2 - \frac{\partial \alpha_3}{\partial x_2} d_1 - H_2 \tag{42}$$

Among them,

$$\begin{aligned} H_2 = {} & \tfrac{\partial \alpha_3}{\partial x_1} x_2 + \tfrac{\partial \alpha_3}{\partial x_3} x_4 + \tfrac{\partial \alpha_3}{\partial \hat{a}_1} \dot{\hat{a}}_1 + \tfrac{\partial \alpha_3}{\partial \hat{a}_{21}} \dot{\hat{a}}_{21} + \tfrac{\partial \alpha_3}{\partial \hat{a}_{31}} \dot{\hat{a}}_{31} + \tfrac{\partial \alpha_3}{\partial \hat{D}_{11}} \dot{\hat{D}}_{11} + \tfrac{\partial \alpha_3}{\partial \hat{\tau}_1} \dot{\hat{\tau}}_1 + \tfrac{\partial \alpha_3}{\partial \hat{D}_1} \dot{\hat{D}}_1 \\ & + \tfrac{\partial \alpha_3}{\partial \dot{\hat{\tau}}} \ddot{\hat{\tau}} + \tfrac{\partial \alpha_3}{\partial \dot{\hat{D}}_1} \ddot{\hat{D}}_1 + \tfrac{\partial \alpha_3}{\partial x_d} \dot{x}_d + \tfrac{\partial \alpha_3}{\partial \dot{x}_d} \ddot{x}_d + \tfrac{\partial \alpha_3}{\partial \ddot{x}_d} \dddot{x}_d + \tfrac{\partial \alpha_3}{\partial \dddot{x}_d} \ddddot{x}_d \end{aligned} \tag{43}$$

Let

$$\tau_2 = \frac{1}{b_4} \tag{44}$$

$$u = \hat{\tau}_2 \overline{u} \tag{45}$$

Among them, $\hat{\tau}_2$ is the estimate of τ_2.

The design of finite-time adaptive controller $\overline{u}$ is:

$$\begin{aligned} \overline{u} = {} & -z_3 - \lambda_{12} z_4^{2\beta-1} - s_{12} z_4 - \hat{b}_1 x_1 + \hat{b}_2 x_3 - \hat{b}_3 x_4 - \tanh(\tfrac{z_4}{\varepsilon_3}) \hat{D}_2 + \hat{a}_{11} \tfrac{\partial \alpha_3}{\partial x_2} x_3 - \hat{a}_{22} \tfrac{\partial \alpha_3}{\partial x_2} x_1 \\ & - \hat{a}_{32} \tfrac{\partial \alpha_3}{\partial x_2} x_2 - \tfrac{\partial \alpha_3}{\partial x_2} \tanh[\tfrac{(\partial \alpha_3 / \partial x_2) z_4}{\varepsilon_4}] \hat{D}_{12} + H_2 \end{aligned} \tag{46}$$

Among them, λ_{12} and s_{12} are normal numbers, $\hat{b}_1$ is the estimate of b_1, $\hat{b}_2$ is the estimate of b_2, $\hat{b}_3$ is the estimate of b_3, $\hat{D}_2$ is the estimate of D_2, $\hat{a}_{11}$ is the estimate of a_1, $\hat{a}_{22}$ is the estimate of a_2, $\hat{a}_{32}$ is the estimate of a_3, $\hat{D}_{12}$ is the estimate of D_1, ε_3 and ε_4 are any normal numbers.

The Lyapunov function for constructing this step is:

$$\begin{aligned} V_4 = {} & V_3 + \tfrac{1}{2} z_4^2 + \tfrac{b_4}{2\gamma_9} \tilde{\tau}_2^2 + \tfrac{1}{2\gamma_{10}} \tilde{b}_1^2 + \tfrac{1}{2\gamma_{11}} \tilde{b}_2^2 + \tfrac{1}{2\gamma_{12}} \tilde{b}_3^2 + \tfrac{1}{2\gamma_{13}} \tilde{D}_2^2 + \tfrac{1}{2\gamma_{14}} \tilde{a}_{11}^2 \\ & + \tfrac{1}{2\gamma_{15}} \tilde{a}_{22}^2 + \tfrac{1}{2\gamma_{16}} \tilde{a}_{32}^2 + \tfrac{1}{2\gamma_{17}} \tilde{D}_{12}^2 \end{aligned} \tag{47}$$

Among them, $\gamma_9 - \gamma_{17}$ are normal numbers, $\tilde{\tau}_2 = \tau_2 - \hat{\tau}_2$, $\tilde{b}_1 = b_1 - \hat{b}_1$, $\tilde{b}_2 = b_2 - \hat{b}_2$, $\tilde{b}_3 = b_3 - \hat{b}_3$, $\tilde{D}_2 = D_2 - \hat{D}_2$, $\tilde{a}_{11} = a_1 - \hat{a}_{11}$, $\tilde{a}_{22} = a_2 - \hat{a}_{22}$, $\tilde{a}_{32} = a_3 - \hat{a}_{32}$, $\tilde{D}_{12} = D_1 - \hat{D}_{12}$.

Updating the laws of design parameters is shown as follows:

$$\dot{\hat{\tau}}_2 = -\gamma_9 z_4 \overline{u} + \gamma_9 \lambda_{13} \tilde{\tau}_2^{2\beta-1} + \gamma_9 s_{13} \tilde{\tau}_2 \tag{48}$$

$$\dot{\hat{b}}_1 = \gamma_{10} z_4 x_1 + \gamma_{10} \lambda_{14} \tilde{b}_1^{2\beta-1} + \gamma_{10} s_{14} \tilde{b}_1 \tag{49}$$

$$\dot{\hat{b}}_2 = -\gamma_{11} z_4 x_3 + \gamma_{11} \lambda_{15} \tilde{b}_2^{2\beta-1} + \gamma_{11} s_{15} \tilde{b}_2 \tag{50}$$

$$\dot{\hat{b}}_3 = -\gamma_{12} z_4 x_4 + \gamma_{12} \lambda_{16} \tilde{b}_3^{2\beta-1} + \gamma_{12} s_{16} \tilde{b}_3 \tag{51}$$

$$\dot{\hat{D}}_2 = \gamma_{13} z_4 \tanh(\frac{z_4}{\varepsilon_3}) + \gamma_{13} \lambda_{17} \tilde{D}_2^{2\beta-1} + \gamma_{13} s_{17} \tilde{D}_2 \tag{52}$$

$$\dot{\hat{a}}_{11} = -\gamma_{14} z_4 \frac{\partial \alpha_3}{\partial x_2} x_3 + \gamma_{14} \lambda_{18} \tilde{a}_{11}^{2\beta-1} + \gamma_{14} s_{18} \tilde{a}_{11} \tag{53}$$

$$\dot{\hat{a}}_{22} = \gamma_{15} z_4 \frac{\partial \alpha_3}{\partial x_2} x_1 + \gamma_{15}\lambda_{19}\widetilde{a}_{22}^{2\beta-1} + \gamma_{15}s_{19}\widetilde{a}_{22} \tag{54}$$

$$\dot{\hat{a}}_{32} = \gamma_{16} z_4 \frac{\partial \alpha_3}{\partial x_2} x_2 + \gamma_{16}\lambda_{20}\widetilde{a}_{32}^{2\beta-1} + \gamma_{16}s_{20}\widetilde{a}_{32} \tag{55}$$

$$\dot{\hat{D}}_{12} = \gamma_{17} z_4 \frac{\partial \alpha_3}{\partial x_2} \tanh[\frac{(\partial\alpha_3/\partial x_2)z_4}{\varepsilon_4}] + \gamma_{17}\lambda_{21}\widetilde{D}_{12} + \gamma_{17}s_{21}\widetilde{D}_{12} \tag{56}$$

Among them, $\lambda_{13} - \lambda_{21}$ and $s_{13} - s_{21}$ are normal numbers.

Similar to Step 3, we end up with:

$$\begin{aligned}
\dot{V}_4 \quad & \le -\lambda_1 z_1^{2\beta} - \lambda_2 z_2^{2\beta} - a_1\lambda_3\widetilde{\tau}_1^{2\beta} - \lambda_4\widetilde{a}_2^{2\beta} - \lambda_5\widetilde{a}_3^{2\beta} - \lambda_6\widetilde{D}_1^{2\beta} - \lambda_7 z_3^{2\beta} - \lambda_8\widetilde{a}_1^{2\beta} - \lambda_9\widetilde{a}_{21}^{2\beta} \\
& -\lambda_{10}\widetilde{a}_{31}^{2\beta} - \lambda_{11}\widetilde{D}_{11}^{2\beta} - \lambda_{12} z_4^{2\beta} - b_4\lambda_{13}\widetilde{\tau}_2^{2\beta} - \lambda_{14}\widetilde{b}_1^{2\beta} - \lambda_{15}\widetilde{b}_2^{2\beta} - \lambda_{16}\widetilde{b}_3^{2\beta} - \lambda_{17}\widetilde{D}_2^{2\beta} - \lambda_{18}\widetilde{a}_{11}^{2\beta} \\
& -\lambda_{19}\widetilde{a}_{22}^{2\beta} - \lambda_{20}\widetilde{a}_{32}^{2\beta} - \lambda_{21}\widetilde{D}_{12}^{2\beta} - s_1 z_2^2 - s_2 z_2^2 - a_1 s_3\widetilde{\tau}_1^2 - s_4\widetilde{a}_2^2 - s_5\widetilde{a}_3^2 - s_6\widetilde{D}_1^2 - s_7 z_3^2 \\
& -s_8\widetilde{a}_1^2 - s_9\widetilde{a}_{21}^2 - s_{10}\widetilde{a}_{31}^2 - s_{11}\widetilde{D}_{11}^2 - s_{12} z_4^2 - b_4 s_{13}\widetilde{\tau}_2^2 - s_{14}\widetilde{b}_1^2 - s_{15}\widetilde{b}_2^2 - s_{16}\widetilde{b}_3^2 - s_{17}\widetilde{D}_2^2 \\
& -s_{18}\widetilde{a}_{11}^2 - s_{19}\widetilde{a}_{22}^2 - s_{20}\widetilde{a}_{32}^2 - s_{21}\widetilde{D}_{12}^2 + 0.2785(\varepsilon_1+\varepsilon_2+\varepsilon_4)D_1 + 0.2785\varepsilon_3 D_2
\end{aligned} \tag{57}$$

3.2. Stability Analysis

According to references [37,38], there are the following criteria:

Theorem 1. *If there exists a continuously differentiable function $L\colon p \to R$, such that it satisfies the following conditions:*

(1) Lis positive definite.

(2) The existence of positive real numbers $q > 0$ and $e \in (0, 1)$, and the existence of an open neighborhood $p_0 \subset p$ containing the origin, makes the following true:

$$\dot{L}(x) + qV^e(x) \le 0, x \in p_0 \backslash \{0\} \tag{58}$$

If $p = p_0 = R^n$, then it is globally finitely time-stable.

From Equations (12), (21), (34) and (47), we can see:

$$\begin{aligned}
V_4 \quad & = \tfrac{1}{2}z_1^2 + \tfrac{1}{2}z_2^2 + \tfrac{a_1}{2\gamma_1}\widetilde{\tau}_1^2 + \tfrac{1}{2\gamma_2}\widetilde{a}_2^2 + \tfrac{1}{2\gamma_3}\widetilde{a}_3^2 + \tfrac{1}{2\gamma_4}\widetilde{D}_1^2 + \tfrac{1}{2}z_3^2 + \tfrac{1}{2\gamma_5}\widetilde{a}_1^2 + \tfrac{1}{2\gamma_6}\widetilde{a}_{21}^2 \\
& + \tfrac{1}{2\gamma_7}\widetilde{a}_{31}^2 + \tfrac{1}{2\gamma_8}\widetilde{D}_{11}^2 + \tfrac{1}{2}z_4^2 + \tfrac{b_4}{2\gamma_9}\widetilde{\tau}_2^2 + \tfrac{1}{2\gamma_{10}}\widetilde{b}_1^2 + \tfrac{1}{2\gamma_{11}}\widetilde{b}_2^2 + \tfrac{1}{2\gamma_{12}}\widetilde{b}_3^2 + \tfrac{1}{2\gamma_{13}}\widetilde{D}_2^2 \\
& + \tfrac{1}{2\gamma_{14}}\widetilde{a}_{11}^2 + \tfrac{1}{2\gamma_{15}}\widetilde{a}_{22}^2 + \tfrac{1}{2\gamma_{16}}\widetilde{a}_{32}^2 + \tfrac{1}{2\gamma_{17}}\widetilde{D}_{12}^2
\end{aligned} \tag{59}$$

According to Section 3.1, V_4 is a continuously differentiable function and a positive definite function.

Let

$$V_4 = V \tag{60}$$

It can be obtained from Equation (57):

$$\begin{aligned}
\dot{V}_4 \quad & \le -\lambda_1 z_1^{2\beta} - \lambda_2 z_2^{2\beta} - a_1\lambda_3\widetilde{\tau}_1^{2\beta} - \lambda_4\widetilde{a}_2^{2\beta} - \lambda_5\widetilde{a}_3^{2\beta} - \lambda_6\widetilde{D}_1^{2\beta} - \lambda_7 z_3^{2\beta} - \lambda_8\widetilde{a}_1^{2\beta} - \lambda_9\widetilde{a}_{21}^{2\beta} \\
& -\lambda_{10}\widetilde{a}_{31}^{2\beta} - \lambda_{11}\widetilde{D}_{11}^{2\beta} - \lambda_{12} z_4^{2\beta} - b_4\lambda_{13}\widetilde{\tau}_2^{2\beta} - \lambda_{14}\widetilde{b}_1^{2\beta} - \lambda_{15}\widetilde{b}_2^{2\beta} - \lambda_{16}\widetilde{b}_3^{2\beta} - \lambda_{17}\widetilde{D}_2^{2\beta} - \lambda_{18}\widetilde{a}_{11}^{2\beta} \\
& -\lambda_{19}\widetilde{a}_{22}^{2\beta} - \lambda_{20}\widetilde{a}_{32}^{2\beta} - \lambda_{21}\widetilde{D}_{12}^{2\beta} - s_1 z_2^2 - s_2 z_2^2 - a_1 s_3\widetilde{\tau}_1^2 - s_4\widetilde{a}_2^2 - s_5\widetilde{a}_3^2 - s_6\widetilde{D}_1^2 - s_7 z_3^2 - s_8\widetilde{a}_1^2 \\
& -s_9\widetilde{a}_{21}^2 - s_{10}\widetilde{a}_{31}^2 - s_{11}\widetilde{D}_{11}^2 - s_{12} z_4^2 - b_4 s_{13}\widetilde{\tau}_2^2 - s_{14}\widetilde{b}_1^2 - s_{15}\widetilde{b}_2^2 - s_{16}\widetilde{b}_3^2 - s_{17}\widetilde{D}_2^2 - s_{18}\widetilde{a}_{11}^2 \\
& -s_{19}\widetilde{a}_{22}^2 - s_{20}\widetilde{a}_{32}^2 - s_{21}\widetilde{D}_{12}^2 + 0.2785(\varepsilon_1+\varepsilon_2+\varepsilon_4)D_1 + 0.2785\varepsilon_3 D_2 \\
& \le -aV - bV^\beta + c
\end{aligned} \tag{61}$$

Among them,

$$a = \min\begin{bmatrix} s_1, s_2, s_3, s_4, s_5, s_6, s_7, s_8, s_9, s_{10}, s_{11}, \\ s_{12}, s_{13}, s_{14}, s_{15}, s_{16}, s_{17}, s_{18}, s_{19}, s_{20}, s_{21} \end{bmatrix} \tag{62}$$

$$b = \min\begin{bmatrix} \lambda_1 2^{\beta-1}, \lambda_2 2^{\beta-1}, \lambda_3 2^{\beta-1}, \lambda_4 2^{\beta-1}, \lambda_5 2^{\beta-1}, \lambda_6 2^{\beta-1}, \lambda_7 2^{\beta-1}, \\ \lambda_8 2^{\beta-1}, \lambda_9 2^{\beta-1}, \lambda_{10} 2^{\beta-1}, \lambda_{11} 2^{\beta-1}, \lambda_{12} 2^{\beta-1}, \lambda_{13} 2^{\beta-1}, \lambda_{14} 2^{\beta-1}, \\ \lambda_{15} 2^{\beta-1}, \lambda_{16} 2^{\beta-1}, \lambda_{17} 2^{\beta-1}, \lambda_{18} 2^{\beta-1}, \lambda_{19} 2^{\beta-1}, \lambda_{20} 2^{\beta-1}, \lambda_{21} 2^{\beta-1} \end{bmatrix} \tag{63}$$

$$c = 0.2785(\varepsilon_1 + \varepsilon_2 + \varepsilon_4)D_1 + 0.2785\varepsilon_3 D_2 \tag{64}$$

Thus, $\widetilde{\tau}_1$, $\widetilde{a}_2$, $\widetilde{a}_3$, $\widetilde{D}_1$, $\widetilde{a}_1$, $\widetilde{a}_{21}$, $\widetilde{a}_{31}$, $\widetilde{D}_{11}$, $\widetilde{\tau}_2$, $\widetilde{b}_1$, $\widetilde{b}_2$, $\widetilde{b}_3$, $\widetilde{D}_2$, $\widetilde{a}_{11}$, $\widetilde{a}_{22}$, $\widetilde{a}_{32}$, $\widetilde{D}_{12}$, z_1, z_2, z_3, and z_4 are all bounded, and the estimated parameters obtained by the parameter-updating laws are all bounded. Since z_1 is bounded in formula (9), and the target value x_d is also bounded, it follows that x_1 is also bounded. In formulas (10) and (11), since z_1 and z_2 are bounded, and the control law α_1 and the target value x_d are also bounded, x_2 is also bounded. In Formulas (16), (17), (19), and (20), since $\widetilde{\tau}_1$, $\widetilde{a}_2$, $\widetilde{a}_3$, $\widetilde{D}_1$, z_1, z_2, and z_3 are bounded, x_3 is also bounded. In Formulas (31), (32), and (35), since $\widetilde{a}_1$, $\widetilde{a}_{21}$, $\widetilde{a}_{31}$, $\widetilde{D}_{11}$, z_1, z_2, z_3, and z_4 are bounded, x_4 is also bounded. In Formulas (45) and (46), since $\widetilde{\tau}_2$, $\widetilde{b}_1$, $\widetilde{b}_2$, $\widetilde{b}_3$, $\widetilde{D}_2$, $\widetilde{a}_{11}$, $\widetilde{a}_{22}$, $\widetilde{a}_{32}$, and $\widetilde{D}_{12}$ are all bounded, it can be judged that u is also bounded. Therefore, all closed-loop signals are bounded.

4. Simulation Results and Discussion

In order to verify the effectiveness of the finite-time adaptive controller designed in this paper, it is simulated and analyzed in this section. The object considered in this paper is EHB gear-drive servo system, and the simulation parameters set in establishing the simulation model are shown in Table 1.

Table 1. Simulation parameters of gear-drive servo system.

Symbol	Parameter	Value	Units
J_l	moment of inertia of the driven side	0.52	kg·m^2
J_m	driving side moment of inertia	0.21	kg·m^2
C_l	viscous friction on the driven side	0.124	Nm/rad
C_m	driving side viscous friction coefficient	0.11	Nm/rad
k_d	stiffness coefficient	0.33	Nm/rad
β_l	break point	0.062	rad
β_r	break point	0.051	rad

In the simulation experiment, in order to verify the position-tracking effect of the controller, we set up two sets of experiments based on MATLAB/Simulink for verification. In experiment 1, we set the expected value of x_d to be a half-sinusoidal signal, and the sinusoidal disturbance term was added to simulate the influence of unknown disturbance on the control effect. In experiment 2, the expected value x_d was set as the ramp signal, and the proportional disturbance term was added to simulate the influence of unknown disturbance on the control effect.

4.1. Experiment 1

The control objective of this paper is the position-tracking target value of the driven side gear of the gear transmission servo system, that is, the state quantity x_1 tracks the target value x_d, and the tracking effect is shown in Figure 4. The arrows show the location-tracking details at the peak. It can be seen from the figure that the tracking effect is good, the convergence rate is fast, and the maximum error is less than 0.1 rad. The effect of gap nonlinearity and unknown interference is compensated, which can meet the demand of position accuracy.

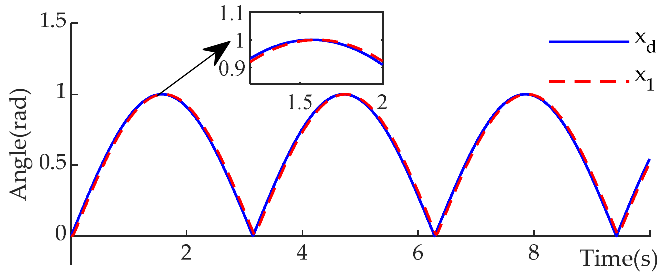

Figure 4. Position-tracking effect under half-sinusoidal input.

In order to observe the difference between the finite-time adaptive controller designed in this paper and the adaptive controller, the error z_1 under the control of each controller is compared. As shown in Figure 5. As can be seen from the figure, the finite-time adaptive controller has smaller overshoot, shorter convergence time and higher control accuracy than the adaptive controller. Compared with literature [27], the convergence rate of tracking error under the control strategy in this paper is faster.

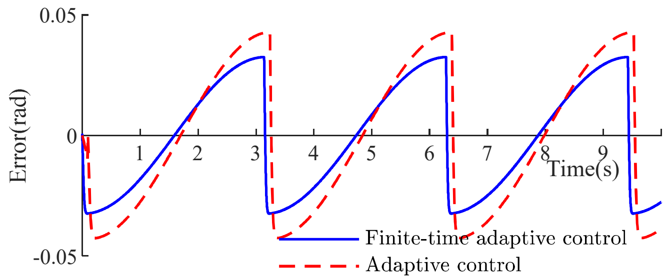

Figure 5. Error z_1 under half-sinusoidal input.

The acceleration of the driven side gear under the half-sinusoidal input condition is shown in Figure 6. From the figure we can see that the acceleration is in the ideal range.

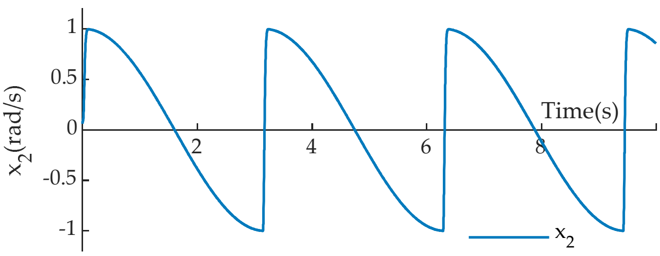

Figure 6. Acceleration of the driven side gear under half-sinusoidal input.

Figure 7 show the changes of estimated parameters of EHB gear-drive servo system. As can be seen from the figure, the estimated parameters of the system rapidly converge to a certain value and change in a small range with the change of the expected value of x_d. This means that the system parameters change while the system is running. At the same time, the validity of the parameter-update laws designed in this paper is proved.

In order to study the effect of parameter β on the convergence rate, we set the value of β to 0.6, 0.7 and 0.67, respectively. As shown in Figure 8. The arrows show the location-tracking details at the peak. As can be seen from the figure, the convergence rate is different when β takes different values. When the value of β is 0.67, the overshoot is the smallest and the convergence is the fastest.

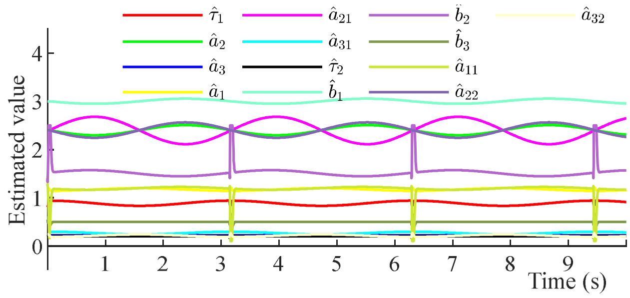

Figure 7. System parameter estimates under half-sinusoidal input.

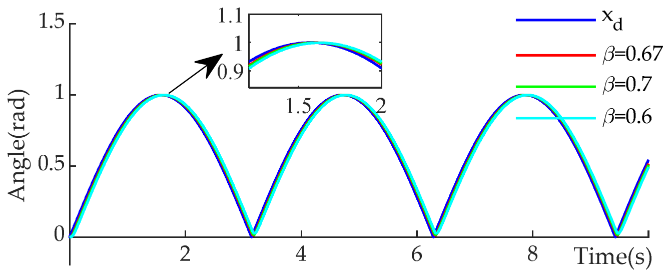

Figure 8. Influence of parameter β on tracking effect under half-sinusoidal input.

As can be seen from the above figures, the EHB gear transmission system parameters will change when working. The updated laws of the parameters designed in this paper can make the estimated parameters converge to a certain range in a certain time and adjust it adaptively according to the working conditions. The finite-time adaptive controller can effectively compensate the effects of unknown interference and dead-zone problems.

4.2. Experiment 2

In order to verify the control effect of the finite-time adaptive controller during fast braking, the expected value x_d is set as the ramp signal. The ramp signal is set to rise from 1s, with a slope of 5 and a final value of 1. As can be seen from Figure 9, the convergence rate of the driven side gear x_1 tracking expected value x_d is faster. We can see from the enlarged figure at the arrow that the maximum error is less than 0.1 rad, which can meet the requirements of control accuracy. The effect of dead zone and unknown interference is compensated effectively, and the control effect is ideal.

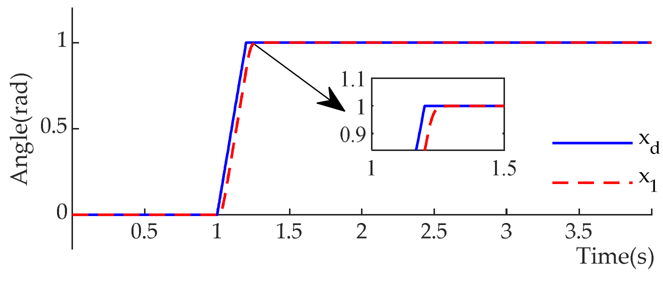

Figure 9. Position-tracking effect under ramp input.

In order to observe the superiority of the finite-time adaptive controller over the adaptive controller, the error z_1 of each controller is compared, as shown in Figure 10. It can be seen from the figure that the finite-time adaptive controller has less overshoot than the adaptive controller. The overshoot is reduced by about 0.05 rad, which is about 30 percent of the overshoot of the adaptive controller. The convergence rate of the finite-time adaptive controller is faster than that of the adaptive controller. It can be verified that the control strategy designed in this paper has better control effects and higher precision. Compared with the tracking error under adaptive control in the literature [33], the tracking error under the control strategy in this paper can be guaranteed to converge to a certain range within a certain period of time.

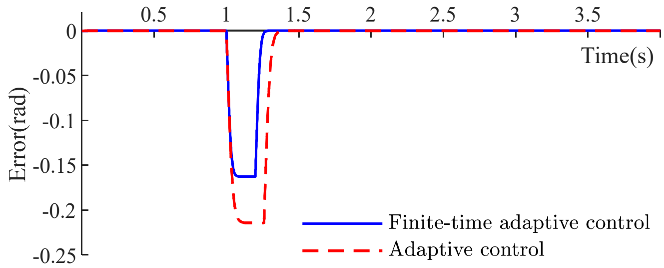

Figure 10. Error z_1 under ramp input.

The acceleration x_2 of the driven side gear is shown in Figure 11. It can be seen from the figure that the convergence rate is fast, and the control effect is excellent.

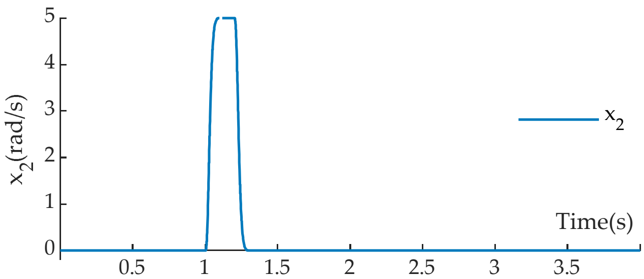

Figure 11. Acceleration of the driven side gear under ramp input.

Figure 12 shows the change in the estimated parameters of the EHB gear-drive servo system under the ramp input. As can be seen from the figure, the estimated parameters of the system will also change with the change in working conditions. A change in the expected value x_d at 1s results in a change in the parameter-update law. When the expected value x_d is stabilized, the new law of the parameters also converges to a certain range. This verifies the validity of the parameter-updating law designed in this paper.

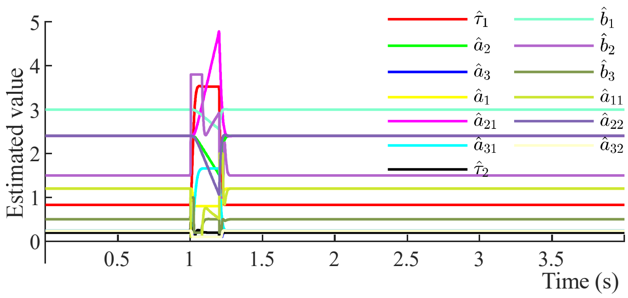

Figure 12. System parameter estimates under ramp input.

In order to study the effect of parameter β on the convergence rate under the ramp input condition, we set β values to 0.6, 0.7 and 0.67, respectively, as shown in Figure 13. It can be seen from the figure that parameter β has a significant effect on the convergence rate. As can be seen from the enlarged figure at the arrow, convergence is fastest when the value of β is 0.67. At the same time, it is proved that the finite-time adaptive controller designed in this paper is effective in improving the convergence rate.

The simulation results show that the control strategy designed in this paper can make the driven side gear of the EHB gear-drive servo system reach the desired position in a limited time and can meet the requirements of position accuracy.

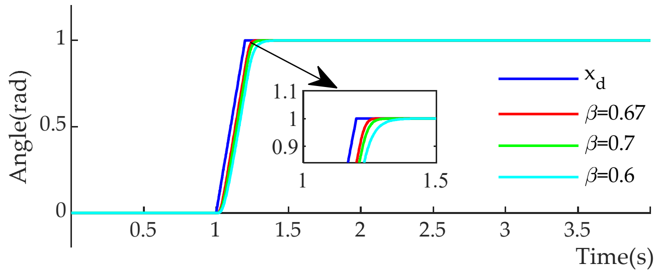

Figure 13. Influence of parameter β on tracking effect under ramp input.

5. Implementation and Results of the HIL Test

In Section 4, simulation tests are carried out to prove the effectiveness of the control strategy designed in this paper. However, the control effect in actual engineering needs further verification, so the HIL test is carried out in this section.

Figure 14 displays the HIL test platform, which is based on NI-PXI and dSPACE. Measuring the position of the gear-drive servo system presents a challenge. However, since the driving side gear is coaxial with the permanent magnet synchronous motor, we can derive the motor rotor's position information from the Hall sensor. This, in turn, provides us with the position information of the driving side gear. Utilizing the transmission relationship, we can calculate the position information of the driven side gear based on the displacement of the master-cylinder push rod. The displacement data of the master-cylinder push rod are obtained from the pulse width modulation signal generated by the digital sensor. By applying the above position relationships and conversions, we acquire the position information of the gear-drive servo system. This information serves to validate the effectiveness of the control strategy proposed in this paper.

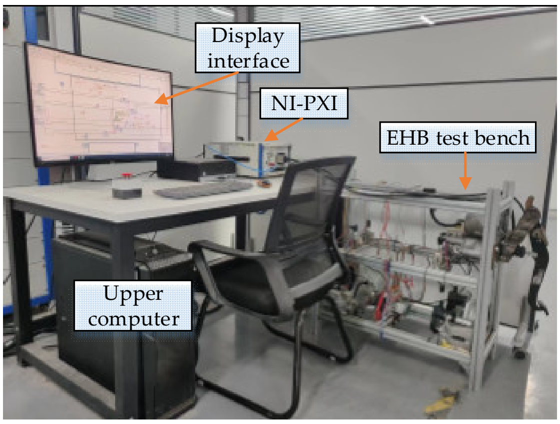

Figure 14. HIL test platform.

In HIL test 1, we set up a half-sine tracking experiment with an amplitude of 2 rad and a period of πs, as shown in Figure 15. Figure 15a shows the displacement y of the master-cylinder push rod, with a peak value of about 1.6 mm. The angle of the driven side gear can be obtained from the transmission relation $y = (s/2\pi)x_1$, where s is the lead of the ball screw mechanism, and $s = 5$. Figure 15b shows the rotation angle of the driving side gear, and it can be seen that its peak value is about 40 rad. It can be seen from Figure 15c that the angle of the driven side gear has a good tracking effect, and the maximum error is less than 0.1 rad. The effect caused by the dead zone is compensated effectively, the control effect is good, and the convergence rate is fast.

To further verify the effectiveness of the control strategy designed in this paper, we designed the amplitudes as 4 rad and 6 rad (see Figures 16 and 17). It can be seen from the two figures that the maximum error of the angle of the driven side gear is less than 0.2 rad when tracking the expected value, and the convergence rate is faster. Under the condition of unknown parameters, unknown disturbance and the dead zone, the finite-time adaptive controller designed in this paper can achieve a relatively stable control effect and can meet the position-tracking requirements of the EHB gear-drive servo system.

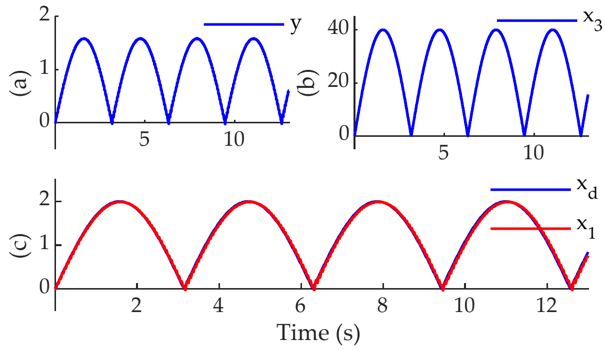

Figure 15. HIL test 1. (**a**) Master-cylinder push rod displacement (mm). (**b**) Drive side gear angle (rad). (**c**) Expected value and driven side gear angle (rad).

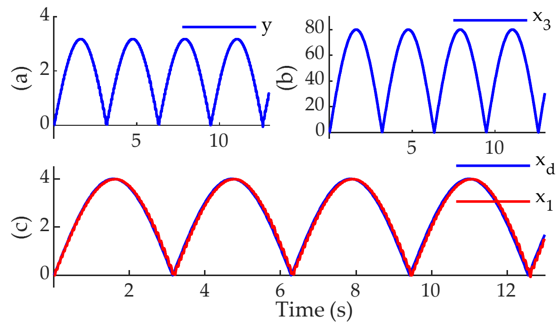

Figure 16. HIL test 2. (**a**) Master-cylinder push rod displacement (mm). (**b**) Drive side gear angle (rad). (**c**) Expected value and driven side gear angle (rad).

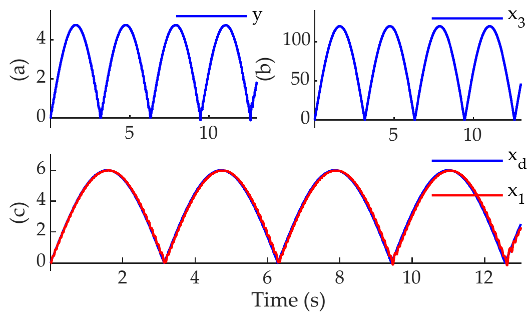

Figure 17. HIL test 3. (**a**) Master-cylinder push rod displacement (mm). (**b**) Drive side gear angle (rad). (**c**) Expected value and driven side gear angle (rad).

Through the HIL test, we have verified that the control strategy proposed in this paper can effectively compensate for the influence of unknown parameters, unknown disturbances, and dead zones. Based on the above analysis, it is evident that the control strategy presented in this paper is effective and capable of enhancing tracking accuracy and convergence rate.

6. Conclusions

In this paper, the backlash nonlinearity of EHB gear-drive servo system is analyzed, and the symmetric dead-zone model of an EHB gear drive is established. Secondly, by combining the finite-time control theory with the adaptive control theory, the parameter-update laws and control laws are designed for the uncertain parameters and dead-zone problems of the system, and boundary estimates are introduced to compensate for the unknown disturbance. Then the stability analysis is carried out to prove that all closed-loop signals are bounded. Finally, simulation and an HIL test are carried out, and the results show that the finite-time adaptive controller designed in this paper is effective.

In future work, the command filtering technology can be introduced to reduce the complexity of the operation and avoid the problem of data explosion. If the conditions permit, the actual vehicle test can be further conducted to verify the practicability of the control strategy.

Author Contributions: Conceptualization, J.W. and S.W.; writing—original draft preparation, S.W.; writing—review and editing, J.W., S.W. and Q.C.; methodology, J.W. and S.W.; data curation, S.W.; software, S.W. and F.M.; visualization, J.W.; formal analysis, Q.C. and F.M. All authors have read and agreed to the published version of the manuscript.

Funding: This research was funded by Shandong Provincial Higher School Youth Innovation Technology Project of China, grant number 2021KJ039.

Data Availability Statement: Not applicable.

Conflicts of Interest: The authors declare no conflict of interest.

References

1. Xiang, W.; Richardson, P.C.; Zhao, C.; Mohammad, S. Automobile brake-by-wire control system design and analysis. *IEEE Trans. Veh. Technol.* **2008**, *57*, 138–145. [CrossRef]
2. Milanés, V.; González, C.; Naranjo, J.E.; Onieva, E.; De Pedro, T. Electro-hydraulic braking system for autonomous vehicles. *Int. J. Automot. Technol.* **2010**, *11*, 89–95. [CrossRef]
3. Yeo, H.; Koo, C.; Jung, W.; Kim, D.; Cheon, J.S. *Development of Smart Booster Brake Systems for Regenerative Brake Cooperative Control*; 0148-7191; SAE Technical Paper; SAE International: Warrendale, PA, USA, 2011.
4. Feigel, H.-J. Integrated brake system without compromises in functionality. *ATZ Worldw.* **2012**, *114*, 46–50. [CrossRef]
5. Tan, Z.-H.; Chen, Z.-F.; Pei, X.-F.; Guo, X.-X.; Pei, S.-H. Development of integrated electro-hydraulic braking system and its ABS application. *Int. J. Precis. Eng. Manuf.* **2016**, *17*, 337–346. [CrossRef]
6. Yu, Z.; Xu, S.; Xiong, L.; Han, W. *An Integrated-Electro-Hydraulic Brake System for Active Safety*; 0148-7191; SAE Technical Paper; SAE International: Warrendale, PA, USA, 2016.
7. Zhao, J.; Hu, Z.; Zhu, B. *Pressure Control for Hydraulic Brake System Equipped with an Electro-Mechanical Brake Booster*; 0148-7191; SAE Technical Paper; SAE International: Warrendale, PA, USA, 2018.
8. Liu, S.; Zhang, L.; Niu, B.; Zhao, X.; Ahmad, A.M. Adaptive neural finite-time hierarchical sliding mode control of uncertain under-actuated switched nonlinear systems with backlash-like hysteresis. *Inf. Sci.* **2022**, *599*, 147–169. [CrossRef]
9. Cao, Z.; Niu, B.; Zong, G.; Xu, N. Small-gain technique-based adaptive output constrained control design of switched networked nonlinear systems via event-triggered communications. *Nonlinear Anal. Hybrid Syst.* **2023**, *47*, 101299. [CrossRef]
10. Theodorakopoulos, A.; Rovithakis, G.A. Guaranteeing preselected tracking quality for uncertain strict-feedback systems with deadzone input nonlinearity and disturbances via low-complexity control. *Automatica* **2015**, *54*, 135–145. [CrossRef]
11. Tarbouriech, S.; Prieur, C.; Queinnec, I. Stability analysis for linear systems with input backlash through sufficient LMI conditions. *Automatica* **2010**, *46*, 1911–1915. [CrossRef]
12. Li, M.; Chen, H.; Zhang, R. An input dead zones considered adaptive fuzzy control approach for double pendulum cranes with variable rope lengths. *IEEE/ASME Trans. Mechatron.* **2022**, *27*, 3385–3396. [CrossRef]
13. Margielewicz, J.; Gąska, D.; Litak, G. Modelling of the gear backlash. *Nonlinear Dyn.* **2019**, *97*, 355–368. [CrossRef]
14. Vörös, J. Modeling and identification of systems with backlash. *Automatica* **2010**, *46*, 369–374. [CrossRef]
15. Corradini, M.L.; Manni, A.; Parlangeli, G. Variable structure control of nonlinear uncertain sandwich systems with nonsmooth nonlinearities. In Proceedings of the 2007 46th IEEE Conference on Decision and Control, New Orleans, LA, USA, 12–14 December 2007; pp. 2023–2028.
16. Shi, Z. Global asymptotic tracking for gear transmission servo systems with differentiable backlash nonlinearity. In Proceedings of the 2014 Seventh International Symposium on Computational Intelligence and Design, Hangzhou, China, 13–14 December 2014; pp. 253–257.
17. Shi, Z.; Zuo, Z. Backstepping control for gear transmission servo systems with backlash nonlinearity. *IEEE Trans. Autom. Sci. Eng.* **2014**, *12*, 752–757. [CrossRef]
18. Zuo, Z.; Ju, X.; Ding, Z. Control of gear transmission servo systems with asymmetric deadzone nonlinearity. *IEEE Trans. Control Syst. Technol.* **2015**, *24*, 1472–1479. [CrossRef]
19. Shi, Z.; Zuo, Z.; Liu, H. Backstepping control for gear transmission servo systems with unknown partially nonsymmetric deadzone nonlinearity. *Proc. Inst. Mech. Eng. Part C J. Mech. Eng. Sci.* **2017**, *231*, 2580–2589. [CrossRef]

20. Lewis, F.L.; Tim, W.K.; Wang, L.-Z.; Li, Z. Deadzone compensation in motion control systems using adaptive fuzzy logic control. *IEEE Trans. Control Syst. Technol.* **1999**, *7*, 731–742. [CrossRef]
21. Zhou, J.; Wen, C.; Zhang, Y. Adaptive output control of nonlinear systems with uncertain dead-zone nonlinearity. *IEEE Trans. Autom. Control* **2006**, *51*, 504–511. [CrossRef]
22. Li, Y.; Tong, S. Adaptive fuzzy output-feedback control of pure-feedback uncertain nonlinear systems with unknown dead zone. *IEEE Trans. Fuzzy Syst.* **2013**, *22*, 1341–1347. [CrossRef]
23. He, X.; Lou, B.; Yang, H.; Lv, C. Robust decision making for autonomous vehicles at highway on-ramps: A constrained adversarial reinforcement learning approach. *IEEE Trans. Intell. Transp. Syst.* **2022**, *24*, 4103–4113. [CrossRef]
24. He, X.; Yang, H.; Hu, Z.; Lv, C. Robust lane change decision making for autonomous vehicles: An observation adversarial reinforcement learning approach. *IEEE Trans. Intell. Veh.* **2022**, *8*, 184–193. [CrossRef]
25. Javaid, U.; Dong, H.; Ijaz, S.; Alkarkhi, T.; Haque, M. High-performance adaptive attitude control of spacecraft with sliding mode disturbance observer. *IEEE Access* **2022**, *10*, 42004–42013. [CrossRef]
26. Xie, B.; Wang, W.; Zuo, Z. Adaptive output feedback control of uncertain gear transmission system with dead zone nonlinearity. In Proceedings of the 2018 13th IEEE Conference on Industrial Electronics and Applications (ICIEA), Wuhan, China, 31 May–2 June 2018; pp. 438–443.
27. Song, J.; Zuo, Z.; Ding, Z. Adaptive backstepping control of gear transmission systems with elastic deadzone. In Proceedings of the 2017 36th Chinese Control Conference (CCC), Dalian, China, 26–28 July 2017; pp. 878–883.
28. Wang, S.; Fan, Z.; Li, B.; Tang, X.; Chen, Z.; Zhou, Q.; Wu, J. Research on adaptive control of input time delay for vehicle electronic stability control system. In Proceedings of the 2022 6th CAA International Conference on Vehicular Control and Intelligence (CVCI), Nanjing, China, 28–30 October 2022; pp. 1–5.
29. Wu, L.-B.; Park, J.H.; Xie, X.-P.; Liu, Y.-J.; Yang, Z.-C. Event-triggered adaptive asymptotic tracking control of uncertain nonlinear systems with unknown dead-zone constraints. *Appl. Math. Comput.* **2020**, *386*, 125528. [CrossRef]
30. Hua, C.; Li, Y.; Guan, X. Finite/fixed-time stabilization for nonlinear interconnected systems with dead-zone input. *IEEE Trans. Autom. Control* **2016**, *62*, 2554–2560. [CrossRef]
31. Bao, J.; Wang, H.; Liu, P.X. Finite-time synchronization control for bilateral teleoperation systems with asymmetric time-varying delay and input dead zone. *IEEE/ASME Trans. Mechatron.* **2020**, *26*, 1570–1580. [CrossRef]
32. Yao, D.; Dou, C.; Zhao, N.; Zhang, T. Finite-time consensus control for a class of multi-agent systems with dead-zone input. *J. Frankl. Inst.* **2021**, *358*, 3512–3529. [CrossRef]
33. Wang, W.; Xie, B.; Zuo, Z.; Fan, H. Adaptive backstepping control of uncertain gear transmission servosystems with asymmetric dead-zone nonlinearity. *IEEE Trans. Ind. Electron.* **2018**, *66*, 3752–3762. [CrossRef]
34. Yin, S.; Shi, P.; Yang, H. Adaptive fuzzy control of strict-feedback nonlinear time-delay systems with unmodeled dynamics. *IEEE Trans. Cybern.* **2015**, *46*, 1926–1938. [CrossRef]
35. Wu, J.; Zhang, J.; Nie, B.; Liu, Y.; He, X. Adaptive control of PMSM servo system for steering-by-wire system with disturbances observation. *IEEE Trans. Transp. Electrif.* **2021**, *8*, 2015–2028. [CrossRef]
36. He, X.; Wu, J.; Huang, Z.; Hu, Z.; Wang, J.; Sangiovanni-Vincentelli, A.; Lv, C. Fear-neuro-inspired reinforcement learning for safe autonomous driving. *IEEE Trans. Pattern Anal. Mach. Intell.* **2023**, 1–13. [CrossRef]
37. Lu, W.; Liu, X.; Chen, T. A note on finite-time and fixed-time stability. *Neural Netw.* **2016**, *81*, 11–15. [CrossRef]
38. Li, X.; Yang, X.; Song, S. Lyapunov conditions for finite-time stability of time-varying time-delay systems. *Automatica* **2019**, *103*, 135–140. [CrossRef]